Novel Natural Product 5,5-*trans*-Lactone Inhibitors of Human α-Thrombin: Mechanism of Action and Structural Studies†

Malcolm P. Weir,*,‡ Susanne S. Bethell,‡ Anne Cleasby,‡ Callum J. Campbell,‡ Richard J. Dennis,‡ Clive J. Dix,‡ Harry Finch,‡ Harren Jhoti,‡ Christopher J. Mooney,‡ Shila Patel,‡ Chi-Man Tang,‡ Malcolm Ward,‡ Alan J. Wonacott,‡ and Christopher W. Wharton§

Glaxo Wellcome Medicines Research Centre, Gunnels Wood Road, Stevenage, Hertfordshire SG1 2NY, U.K., and School of Biochemistry, University of Birmingham, Birmingham B15 2TT, U.K.

Received October 9, 1997; Revised Manuscript Received February 18, 1998

ABSTRACT: High-throughput screening of methanolic extracts from the leaves of the plant *Lantana camara* identified potent inhibitors of human α-thrombin, which were shown to be 5,5-*trans*-fused cyclic lactone euphane triterpenes [O'Neill et al. (1998) *J. Nat. Prod.* (submitted for publication)]. Proflavin displacement studies showed the inhibitors to bind at the active site of α-thrombin and α-chymotrypsin. Kinetic analysis of α-thrombin showed tight-binding reversible competitive inhibition by both compounds, named GR133487 and GR133686, with respective k_{on} values at pH 8.4 of 1.7×10^6 s^{-1} M^{-1} and 4.6×10^6 s^{-1} M^{-1}. Electrospray ionization mass spectrometry of thrombin/inhibitor complexes showed the tight-bound species to be covalently attached, suggesting acyl-enzyme formation by reaction of the active-site Ser195 with the *trans*-lactone carbonyl. X-ray crystal structures of α-thrombin/GR133686 (3.0 Å resolution) and α-thrombin/GR133487 (2.2 Å resolution) complexes showed continuous electron density between Ser195 and the ring-opened lactone carbonyl, demonstrating acyl-enzyme formation. Turnover of inhibitor by α-thrombin was negligible and mass spectrometry of isolated complexes showed that reversal of inhibition occurs by reformation of the *trans*-lactone from the acyl-enzyme.The catalytic triad appears undisrupted and the inhibitor carbonyl occupies the oxyanion hole, suggesting the observed lack of turnover is due to exclusion of water for deacylation. The acyl-enzyme inhibitor hydroxyl is properly positioned for nucleophilic attack on the ester carbonyl and therefore relactonization; furthermore, the higher resolution structure of α-thrombin/GR133487 shows this hydroxyl to be effectively superimposable with the recently proposed deacylating water for peptide substrate hydrolysis [Wilmouth, R. C., et al. (1997) *Nat. Struct. Biol. 4,* 456−462], suggesting the α-thrombin/GR133487 complex may be a good model for this reaction.

α-Thrombin is a serine protease that belongs to the trypsin family and is generated by autocatalytic and factor Xa cleavage of the circulating plasma protein prothrombin at the final step of the coagulation cascade; it has a central role in the hemostatic process, where it displays both coagulant (*3*) and anticoagulant properties (*4*). The major coagulant effects are the cleavage of fibrinogen to release fibrin, the activation of platelets through proteolysis of the platelet thrombin receptor leading to platelet aggregation (*5*), and conversion of factors V and VIII to factors Va and VIIIa, respectively, in a positive feedback loop, causing amplification of the cascade (*3*). X-ray crystallographic studies have shown α-thrombin to possess the classical trypsin-like fold and the Ser195/His57/Asp102[1] catalytic triad at the active site (*6*). In addition, the structure contains insertion loops that help impart specificity by participating in substrate and inhibitor binding as well as a unique secondary binding site, the exosite, which is distant from the active site. α-Thrombin utilizes this secondary site when it binds fibrinogen and the leech anticoagulant protein hirudin in a bidentate manner (*7*). One region of the α-thrombin structure that appears to determine substrate specificity is a loop close to the active site, referred to as the sixties loop, residues from which help define the S1′ and S2 pockets[2] in particular (*9*). The S1 pocket prefers basic residues such as Arg and Lys due to Asp189, which forms the base of the pocket.

Serine proteases have attracted a great deal of interest as drug targets due to their widespread involvement in biological processes, and many serine protease inhibitors have been designed or discovered that exploit the catalytic mechanism to form reversible or irreversible covalent adducts [reviewed by Powers and Harper (*10*) and Wharton (*11*)]. Classes of irreversible inhibitor include β-lactam elastase inhibitors (*12*−*14*), isocoumarins (*15*), isatoic anhydrides (*16*), enol lactones (*17*), ynenol lactones (*18*), 6-chloro-2-pyrones (*19*), and the chloromethyl ketone α-thrombin inhibitor PPACK,[3] which forms an adduct to His57 (*20*). Boronate, trifluo-

† Coordinates have been deposited with the Brookhaven Protein Data Bank under codes 1AWF (GR133487) and 1AWH (GR133686).

‡ Glaxo Wellcome Medicines Research Centre.

§ University of Birmingham.

[1] The amino acid residue numbering follows the chymotrypsinogen system of Bode et al. (*9*).

[2] Naming of enzyme pockets (S1, S2, ...) corresponding to substrate/inhibitor residues (P1, P2, ...) follows the notation of Schechter and Berger (*8*).

S0006-2960(97)02499-9 CCC: $15.00
Published on Web 04/23/1998

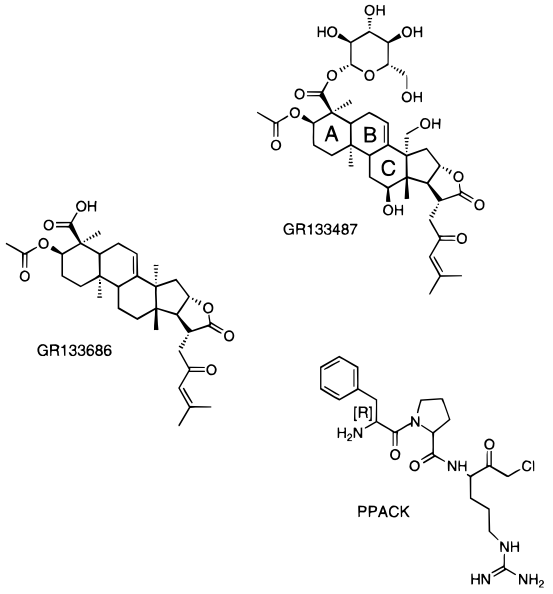

FIGURE 1: Triterpenes GR133686 and GR133487 were isolated from the leaves of the plant *Lantana camara*; extracts of the leaves showed activity as inhibitors of α-thrombin in an in vitro fibrin-formation assay and the active components were purified and characterized from this source as described in O'Neill et al. (*1*). The activity of these compounds against a range of serine proteases is shown in Table 2. The structure of the peptide choloromethyl ketone inhibitor PPACK (*20*) used here for mechanistic studies is shown for comparison.

romethyl ketone, and aldehyde inhibitors have been reported to form reversible covalent adducts to Ser195 that mimic the catalytic tetrahedral intermediate (*21*−*24*). Thrombin's central role in clot formation combined with this high level of knowledge of serine protease inhibition makes it a prime target for antithrombotic inhibitor design, and many inhibitors have been produced both by mechanism-based approaches and by design of competitive inhibitors that bind exclusively by noncovalent interactions (*24*−*27*).

In a search for novel α-thrombin inhibitors by high-throughput screening of natural products, methanolic extracts of leaves from *Lantana camara* (commonly known as wild sage) were found potently to inhibit human α-thrombin and to a lesser extent α-chymotrypsin and other serine proteases; fractionation and purification showed the active constituents to be 5,5-*trans*-fused cyclic lactone euphane triterpenes (Figure 1, *1*). We describe here the structural and mechanistic basis for α-thrombin inhibition by these molecules, which is shown to be via reversible acylation of Ser195 by the lactone moiety and which provides a basis for generalization of this novel template to the design of serine protease inhibitors. In addition, these observations show the precise location of the hydroxyl group for inhibitor deacylation (relactonization), which may coincide with the position of the deacylating water molecule for peptide substrate hydrolysis (*2*).

[3] Abbreviations: EDTA, ethylenediaminetetraacetic acid; ESI-MS, electrospray ionization mass spectrometry; FT-IR, Fourier transform infrared spectroscopy; MS/MS, tandem mass spectrometry; PEG, poly(ethylene glycol); pNA, *p*-nitroanilide; pNp, *p*-nitrophenyl; PPACK, D-Phe-L-Pro-L-Arg chloromethyl ketone; Eoc-, *N*-ethoxycarbonyl; Boc, *tert*-butyloxycarbonyl; boroarginine, boronic acid analogue of arginine; RP-HPLC, reversed-phase high-pressure liquid chromatography; tPA, tissue plasminogen activator.

EXPERIMENTAL PROCEDURES

Materials. Freeze-dried human prothrombin complex intermediate was purchased from Bio Products Laboratory, Dagger Lane, Elstree, U.K. *Oxyuranus scutellatus* snake venom, *N-trans*-cinnamoylimidazole, and sodium phosphate were purchased from Sigma. Bovine pancreatic chymotrypsin, bovine trypsin, and human plasmin were from Sigma; factor Xa was from Boehringer; factors XIa and XIIa were from Enzyme Research Laboratories Inc.; and human tPA, cathepsin G, and neutrophil elastase were from Calbiochem, Nottingham, U.K. Specific peptide *p*-nitroanilide substrates for elastase and cathepsin G were from Sigma; tPA substrate was from American Diagnostica Inc.; and substrates for chymotrypsin, trypsin, factors Xa, XIa, and XIIa, plasmin, and α-thrombin were from Kabivitrum. Ultrapure proflavin hemisulfate was purchased from ICN Biomedicals. The heparin−Sepharose CL-6B resin was from Pharmacia, PEG 6000 was from Fluka, Tris-HCl was from BDH, and the sodium chloride was from Fisons. The euphane triterpene compounds GR133686 and GR133487 (Figure 1) were isolated from the leaves of the *Lantana camara* plant as previously described (*1*). All buffers were made up with Milli-Q-grade water. PPACK was from Calbiochem. Molecular weight cutoff filters were from Millipore, Watford, U.K.

α-Thrombin Activation and Purification. Human α-thrombin was activated and purified following the procedure of Fenton et al. (*28*) and later by the modified procedure of Ngai and Chang (*29*). One vial of the prothrombin complex intermediate was resuspended at room temperature in 20 mM Tris-HCl and 0.1 M NaCl buffer, pH 7.5, and diluted until the concentration of prothrombin was 0.2−0.4 mg/mL, estimated using an extinction coefficient at 280 nm of $\epsilon = 5.2 \times 10^4\ M^{-1}\ cm^{-1}$. The concentration of $CaCl_2$ was made up to 10 mM by adding 1 mL of a 1 M $CaCl_2$ solution per 100 mL of prothrombin solution. Freeze-dried snake venom (10 mg) was dissolved in 1 mL of water and added to the prothrombin under constant stirring. The activation was monitored by the increase in absorbance at 405 nm following the release of nitroaniline from the cleavage of the chromogenic substrate S2238 (*30*). When the rate of absorption change became constant, the activated solution was placed on ice. The activation was usually complete in 30−45 min. The activated α-thrombin was loaded onto a heparin−Sepharose column equilibrated with 20 mM Tris-HCl and 0.1 M NaCl buffer, pH 7.5, at a flow rate of 5 mL/min. After loading, the column was washed until all the unbound inactive material was eluted. The activated α-thrombin was eluted from the column with a linear salt gradient from 0 to 100% of 20 mM Tris-HCl and 1 M NaCl, pH 6.0, and pooled fractions were stored at −70 °C.

Proflavin Binding. Proflavin displacement studies were performed to assess inhibitor active-site binding (*31*). The buffer used was 50 mM sodium phosphate and the pH was either 6.0 or 8.4 and was adjusted by varying the ratio of the mono- and dibasic phosphate salts. Fresh stocks of proflavin were prepared daily and the concentration was determined by measuring the absorption at 444 nm and using an extinction coefficient of $\epsilon = 3.79 \times 10^4\ M^{-1}\ cm^{-1}$. Binding and displacement studies of proflavin to α-thrombin were conducted on a double-beam Cecil 6600 instrument

with a thermostated 10 mm path length cuvette holder to which a Julabo U3 circulating water bath was attached and set at 25 °C. The binding studies were conducted by adding proflavin in 0.5 μM increments to the sample and reference cuvettes. The sample cuvette contained 8.8 μM α-thrombin. The displacement experiments were performed by titrating the compound GR133686 into a 10 μM α-thrombin/13 μM proflavin solution.

Fourier Transform Infrared Spectroscopy. The instrument used was a Nicolet 60SX Fourier transform instrument attached to an IBM personal computer running the Nicolet PC/IR software. The cell used was a 75 μm path length, CaF_2 demountable liquid cell with Teflon spacers. The experiments were carried out using bovine pancreatic α-chymotrypsin as a model for thrombin. Protein was dissolved in unbuffered D_2O to give approximately 3 mL of a 50 mg/mL stock solution. After 24−48 h, the pD was adjusted to 7.4 by adding DCl or NaOD. Ten microliters of a 45 mM inhibitor solution in acetonitrile was added over a period of 2 min to give a 1:1 enzyme-to-inhibitor ratio. The reference samples were prepared in similar fashion, leaving out the compound. To ensure that the protein concentration in each sample and reference set was identical, each set was prepared from the same stock, which was centrifuged for 2 min in an Eppendorf centrifuge prior to division into two 0.4 mL aliquots. The sample was loaded into the cell and 3200 scans at 2 cm^{-1} resolution were collected over a period of about 5 min. The reference spectrum was subtracted from that of the sample to give the difference spectrum of the effect of the inhibitor complex. The extent of acylation was monitored independently by titrating a 40 μL aliquot of the sample with *N*-*trans*-cinnamoylimidazole halfway through the data collection (*32*).

Enzyme Kinetics. Inhibition versus a range of serine proteases was initially assessed by 15-min IC_{50} measurements. Enzyme and inhibitor were preincubated in 96-well microplates for 15 min, and reactions were initiated by addition of peptidyl *p*-nitroanilide substrates to a final volume of 200 μL. Activity was measured at 405 nm as the initial rate of substrate hydrolysis, and the concentration of inhibitor reducing activity to 50% of uninhibited control levels (IC_{50}) was determined. Conditions for the following proteases were essentially as described in the associated references: α-thrombin (*33*), tissue plasminogen activator (*34*), factor Xa (*35*), cathepsin G and human neutrophil elastase (*36*), and plasmin (*37*). Conditions and substrates for chymotrypsin, trypsin, factor XIa, and factor XIIa were (a) chymotrypsin, 50 mM Tris-HCl and 50 mM $CaCl_2$, pH 8.4, assayed against 200 μM MeO-Suc-Arg-Pro-Tyr-pNA; (b) trypsin, 50 mM Tris-HCl and 15 mM $CaCl_2$, pH 8.4, assayed against 160 μM *N*-benzoyl-Ile-Glu-Gly-Arg-pNA; (c) factor XIa and factor XIIa, 28 mM barbital, 125 mM NaCl, and 1 mM EDTA, pH 7.4, assayed against 400 μM pyroGlu-Pro-Arg-pNA and 200 μM D-Pro-Phe-Arg-pNA, respectively.

Detailed kinetic analysis of α-thrombin was carried out as follows. Specific chromogenic substrate S2238 was dissolved in water at 2 mM, stored at 4° C, and diluted in the appropriate buffers for use. For experiments at pH 8.4 the buffer was 50 mM Tris-HCl, 0.5 M NaCl, and 0.1% PEG 6000 (K_m = 1.91 μM), and at pH 6.0 the buffer was 50 mM Na_2HPO_4/NaH_2PO_4, 0.75 M NaCl, and 0.1% PEG 6000 (K_m = 10.6 μM). Progress curves were measured at 25 °C in a final volume of 1 mL in 1 cm path length cuvettes at a substrate concentration of 0.2 mM except where stated, and reactions were monitored at 405 nm in a Beckman DU70 spectrophotometer. The molar extinction coefficient was determined at 405 nm using a 0.1 mM *p*-nitroaniline standard (Kabivitrum) as 1.02×10^4 M^{-1} cm^{-1} at pH 6.0 and as 1.0×10^4 M^{-1} cm^{-1} at pH 8.4. These values were used to calculate product release in progress curve experiments.

Enzyme Kinetics: Inhibition Progress Curves. Preliminary experiments indicated that GR133686 and GR133487 displayed time-dependent inhibition of α-thrombin and α-chymotrypsin. Depending on the inhibition mechanism, the *pseudo*-first-order rate constant k_{obs}, estimated from inhibition progress curves, varies with inhibitor concentration [I] in a characteristic fashion (*38*). A linear relationship

Scheme 1

$$E + I \underset{k_{off}}{\overset{k_{on}}{\rightleftharpoons}} EI$$

implies simple time-dependent inhibition (Scheme 1), where k_{obs} has the relationship

$$k_{obs} = k_{off} + k_{on}[I]/(1 + [S]/K_m) \quad (1)$$

A hyperbolic plot of k_{obs} versus [I] indicates a mechanism displaying saturation kinetics typical of alternate substrate or slow-binding inhibition, in which enzyme and inhibitor rapidly equilibrate to form a noncovalent complex, E·I, which then isomerizes relatively slowly to the tight or stable complex, EI* (Scheme 2), where k_{obs} has the relationship

$$k_{obs} = k_4 + k_3[I]/K_i(1 + [S]/K_m + [I]/K_i) \quad (2)$$

k_{off} and k_4 were measured in separate experiments as described below.

Scheme 2

$$E + I \overset{K_i}{\rightleftharpoons} E{\cdot}I \underset{k_4}{\overset{k_3}{\rightleftharpoons}} EI^*$$

Experiments generating progress curve data of the time-dependent inhibition of α-thrombin by GR133487 and GR133686 were initiated by adding 990 μL of a preformed mixture of substrate and inhibitor at varying concentrations to 10 μL of human α-thrombin to give a final concentration of 1 nM α-thrombin. Progress curve data were collected by recording A_{405} for 60 min or for shorter periods at higher inhibitor concentrations and transferred using Beckman data capture software. Experiments were carried out under *pseudo*-first-order conditions ([I] > 25[E]). Control reactions always gave a linear increase in absorbance well in excess of those used for analysis, but typically less than 10% of substrate was consumed. The range of inhibitor concentrations used was defined empirically to give measurable values of k_{obs}.

The integrated rate equation describing product concentration as a function of time in the presence of a slow-binding inhibitor (*38*), eq 3, was fitted to the data of each curve by nonlinear regression using the RS/1 (BBN Software Products Corp.) procedure FITFUNCTION, giving values of k_{obs} at each concentration of inhibitor:

$$A_{405} = v_s t + (v_0 - v_s)(1 - e^{-k_{obs}t})/k_{obs} + c \qquad (3)$$

where v_0 is the initial rate of change of absorbance, v_s is the steady-state rate, k_{obs} is the *pseudo*-first-order rate constant for transition from v_0 to v_s, and c is the initial absorbance at 405 nm.

Enzyme Kinetics: Concentrated Incubations and Dissociation of Preformed Complexes—Measurement of k_4. Thrombin (2 μM) was mixed with an equal volume of GR133487 (2.5 μM at pH 8.4, 10 μM at pH 6.0, for 60 min), or 5 μM thrombin was mixed with an equal volume of GR133686 (20 μM at pH 8.4, 40 μM at pH 6.0, for 60 min). Assay of residual activity of these mixtures confirmed that thrombin activity was minimal. Progress curves of the recovery of enzymatic activity were carried out by extensive dilution into a solution of S2238, 250 μM, and observing the recovery of activity by monitoring absorbance at 405 nm. Final thrombin concentrations were 0.2 nM (GR133487 at pH 8.4), 0.5 nM (GR133487 at pH 6.0), 0.1 nM (GR133686 at pH 8.4), and 0.05 nM (GR133686 at pH 6.0). The low final concentration of α-thrombin for GR133686 at pH 6.0 was necessary because of the much longer time course of recovery that was observed for these conditions. Equation 3 was fitted to the data of individual progress curves to determine k_{obs}, which for convenience is referred to as k_{dis} when obtained from dissociation progress curves. Equations 1 and 2 define k_{dis}. In these experiments the extensive dilutions (4000−100 000-fold) made to allow recovery of total enzyme activity give a low final value of [I]. This combines with a large value of $1 + [S]/K_m$ such that k_{dis} tends to k_{off} (eq 1) or k_4 (eq 2) and thus becomes a direct measure of the limiting dissociation rate constant. That the final concentration of inhibitor was negligible was confirmed for GR133487 at pH 8.4 by performing dissociation experiments over a range of inhibitor concentrations, with no detectable variation in k_{dis}.

Enzyme Kinetics: Residual Activity under Single-Turnover Conditions. Experiments were performed at pH 8.4 by mixing a final concentration of 50 nM GR133487 with increasing amounts of α-thrombin, 10−100 nM, and assaying residual activity at each combination of enzyme:inhibitor at 30, 90, and 180 min after mixing. Over part of the range of this experiment α-thrombin was in significant excess over GR133487, providing several samples under single-turnover conditions.

Formation and Isolation of α-Thrombin/Inhibitor Complexes. α-Thrombin/inhibitor complexes were separated from free inhibitor by ultrafiltration as follows. α-Thrombin, in 300 μL aliquots at a concentration of 16 μM, was buffered with 50 mM Na_2HPO_4/NaH_2PO_4, pH 6, and 0.75 M NaCl. Inhibitors were dissolved in a small amount of CH_3CN followed by excess buffer to a final concentration of 1.6 mM. The incubation solution was prepared by addition to the α-thrombin of 15 μL of inhibitor solution. The vessel was then incubated at 37 °C for 5 min, and 25 μL was removed and injected onto RP-HPLC. The remaining 275 μL was transferred to a centrifugal filtration cartridge with a nominal molecular weight cutoff of 10 000 kDa, which had been prewashed with buffer leaving the membrane just wet, and spun through with further loadings of buffer (2 × 300 μL), leaving around 50 μL each time; after the second wash the volume in the vessel was made back to 300 μL and the total was transferred to a fresh tube. A 25 μL aliquot was subjected to RP-HPLC.

Competitive Incubation with PPACK. One mole equivalent of PPACK dissolved in buffer was added to the remainder of the α-thrombin/inhibitor complex isolated as above. The mixture was incubated at 37 °C and aliquots were chromatographed at hourly intervals from 1 to 4 h after PPACK addition. The eluted components were collected for mass spectrometric analysis. A further aliquot containing a molar excess of fresh thrombin was added to a 50 μL portion of α-thrombin/inhibitor/PPACK incubation mixture at the 4 h time point.

RP-HPLC. Chromatography was carried out using a Pharmacia FPLC system at a flow rate of 1 mL/min on a 4.6 × 100 mm Pharmacia PRO−RPC column using a linear gradient with a 5 min hold time at 5% eluent B followed by 5−60% eluent B over 50 min. Eluent A was 0.1% aqueous trifluoroacetic acid, and eluent B contained 0.1% TFA in 60% CH_3CN/H_2O. Detection was performed at 252 nm; the absorbance ranges are shown in the chromatograms. Samples were dried in a Savant vacuum centrifuge prior to mass spectrometry.

Mass Spectrometry. Mass spectrometry was performed by infusion of the RP-HPLC fractions dissolved in CH_3CN/H_2O/AcOH (50:50:1) at 1 μL/min into an Analytica electospray ionization source fitted to a Finnigan TSQ-700. The mass spectrometer was scanned over the *m*/*z* range 800−1800 for α-thrombin and *m*/*z* 400−800 for the inhibitors. A scan cycle time of 30 s was used. MS/MS experiments utilized unit resolution for parent selection of *m*/*z* 753, and −20 V for collision potential. RP-HPLC/MS data on autolytically cleaved α-thrombin samples was recorded on a Sciex API III mass spectrometer scanned over the range *m*/*z* 900−2400 in 0.3 Da steps at 0.5 ms/step.

X-ray Crystallography: α-Thrombin/GR133686. Human α-thrombin was inhibited using a 1:5 molar ratio of protein to GR133686 dissolved in acetonitrile. Crystallization experiments were performed using vapor diffusion techniques together with the McPherson screen to scan potential conditions (*39*). Crystals suitable for X-ray analysis were grown from 8−12% PEG 4000 and 100 mM sodium acetate, pH 5.0−5.5, at 4 °C using an initial protein concentration of 36 mg/mL. Crystals grew as orthorhombic rods in 7 days to a typical size of 350 × 100 μm and belong to space group $P2_12_12_1$ (a = 65.6 Å, b = 102.8 Å, c = 119.7 Å) with two molecules per asymmetric unit. A data set was collected from one crystal using a FAST area detector system mounted on an Enraf-Nonius FR581 rotating anode and processed using MADNES and CCP4 programs (Table 1, *40*). The structure was solved using molecular replacement techniques with a well-refined 1.9 Å structure of a α-thrombin/PPACK complex (coordinates courtesy of Professor W. Bode, Max Planck Institute, Munich); the search model consisted only of protein atoms. The rotation function using X-PLOR (*41*) resulted in two peaks 7.5σ above the mean using 3−15 Å data. These two orientations were then optimized independently using the X-PLOR Patterson-correlation function. The translation function was then calculated with a data range 3−10 Å and using the two orientations independently; a top peak of ∼13σ resulted in each run. Refinement was performed using X-PLOR and the final *R*-factor was 20.2%

Table 1: Statistics for X-ray Data Collection and Refinement of the α-Thrombin/Inhibitor Complexes

	GR133686	GR133487
	Data Collection	
space group	$P2_12_12_1$	$C2$
unit cell (Å)	$a = 65.6$, $b = 102.8$, $c = 119.7$	$a = 71.9$, $b = 71.8$, $c = 73.0$[a]
resolution (Å)	3.0	2.2
R-merge (%)	12.4	6.0
	Refinement	
model atoms	4840 (2 solvent)	2757 (230 solvent)
R-factor (%)	20.2	19.9
	Geometry[b]	
bonds (Å)	0.017 (0.018)	0.016
angles (deg)	3.6 (3.6)	3.1
dihedrals (deg)	29.9 (30.1)	29.3
impropers (deg)	2.1 (1.9)	1.9

[a] $\beta = 101.4°$. [b] The values in parentheses are for the second molecule in the asymmetric unit for the thrombin/GR133686 complex.

at 3 Å with good stereochemistry for the model (Table 1).

X-ray Crystallography: α-Thrombin/GR133487. Hirugen−thrombin was prepared according to a modification of the method of Skrzypczak-Jankun et al. (*7*). Crystallization was carried out by the vapor diffusion method using 10 mg/mL of hirugen−thrombin inhibited by GR133487 (in excess of 100K_i), 12.5% PEG 4000, 50 mM Hepes, pH 7, and 100 mM NaCl in the drop and 30% PEG 4000, 100 mM Hepes, pH 7, and 1.6 M NaCl in the well. After 24 h equilibration time the drops were seeded with microcrystals of hirugen−thrombin following which the NaCl concentration in the well was slowly increased over several days. Crystals grew at 20 °C to typical sizes of 300 × 300 × 225 μm and were characterized as belonging to space group *C*2 (Table 1). A data set was collected using the in-house FAST area detector (as above) to 2.2 Å resolution using one crystal. The α-thrombin/GR133487 structure did not require a separate structure solution as the crystals were isomorphous to the native hirugen−thrombin structure that had previously been solved using molecular replacement in our laboratory using the α-thrombin/PPACK search model. The refinement was performed using X-PLOR and the final *R*-factor was 19.9% at 2.2 Å with good geometry for the model (Table 1).

RESULTS

The strained nature of the 5,5-*trans*-lactone ring system was suggestive of protease inhibition by ring opening and acylation of the active-site serine. Binding at the active site of α-thrombin and α-chymotrypsin was first shown by displacement of the dye proflavin monitored by difference absorption spectroscopy; proflavin is known to bind in the active site of serine proteases with a low micromolar K_d and with a concomitant shift in absorption maximum from 444 to 465 nm (*31, 42*). It has been shown to bind to an apolar site close to the catalytic site of α-thrombin (*43*). Titration of GR133686 into 10 μM α-thrombin/proflavin complex at pH 8.3 showed displacement of proflavin proportional to inhibitor concentration (Figure 2), indicating tight binding within the mixing time of the experiment (20−30 s). Similar results were seen with thrombin at pH 6 and with α-chymotrypsin. No change in absorbance was seen during 2 h at 20 °C with a 2-fold excess of GR133686 over α-thrombin,

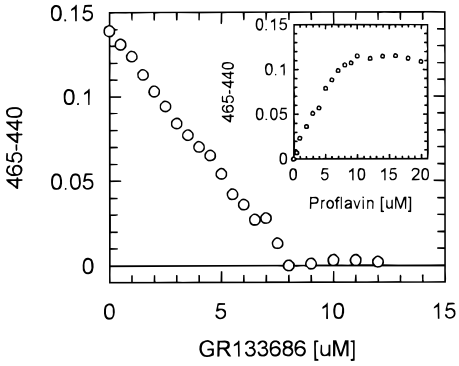

FIGURE 2: Proflavin displacement from α-thrombin by GR133686. Titration of proflavin into a 10 μM solution of α-thrombin causes a stoichiometric change in the (465 − 440 nm) difference absorption of the dye as shown in the inset figure. Proflavin is quantitatively displaced by the tighter-binding GR133686, indicating that the inhibitor binds in the active site of α-thrombin.

Table 2: IC_{50} Data for GR133487 and GR133686 versus a Range of Serine Proteinases

	IC_{50}[a] (μM)	
enzyme	GR133487[a]	GR133686
α-thrombin	0.004	0.004
α-chymotrypsin	0.01	0.07
trypsin	0.12	0.07
tPA	>10	1.0
factor Xa	>10	>10
cathepsin G	>10	2.2
plasmin	5.6	3.5
factor XIa	1.1	0.7
neutrophil elastase	>10	>10
factor XIIa	>10	>10

[a] IC_{50} values (means of three determinations) are the inhibitor concentrations reducing enzyme activity to 50% control level after 15 min.

indicating that the tightly bound complex was relatively stable.

Kinetic Analysis of α-Thrombin Inhibition. The time-dependent onset of inhibition of α-thrombin by GR133487 and GR133686 was initially observed in IC_{50} determinations, which at pH 8.4 also showed that inhibition was tight-binding and selective for α-thrombin over a number of other serine proteases (Table 2), although it is noteworthy that these compounds are also potent α-chymotrypsin inhibitors despite the difference in P1 specificity of these enzymes (*44*).

The kinetics of α-thrombin inhibition were examined in detail. A typical family of inhibition progress curves for GR133487 at pH 8.4 is shown in Figure 3a; similar families of curves were obtained at pH 8.4 for GR133686 and at pH 6.0 for both compounds. GR133686 at pH 6.0 and GR133487 at both pH 6.0 and 8.4 showed evidence of saturation of k_{obs} with [I], as shown in Figure 3b, typical of the Scheme 2 mechanism. GR133686 at pH 8.4, however, showed a linear increase of k_{obs} with [I] and was therefore analyzed according to Scheme 1.

Because of the small magnitude of k_{off} and k_4 compared to k_{obs}, the former parameters were measured directly from dissociation progress curves . In these experiments enzyme and inhibitor were mixed under conditions favoring production of the tight complex, EI*, such that dissociation could be initiated by extensive dilution into a solution of chromogenic substrate with the enzyme almost completely

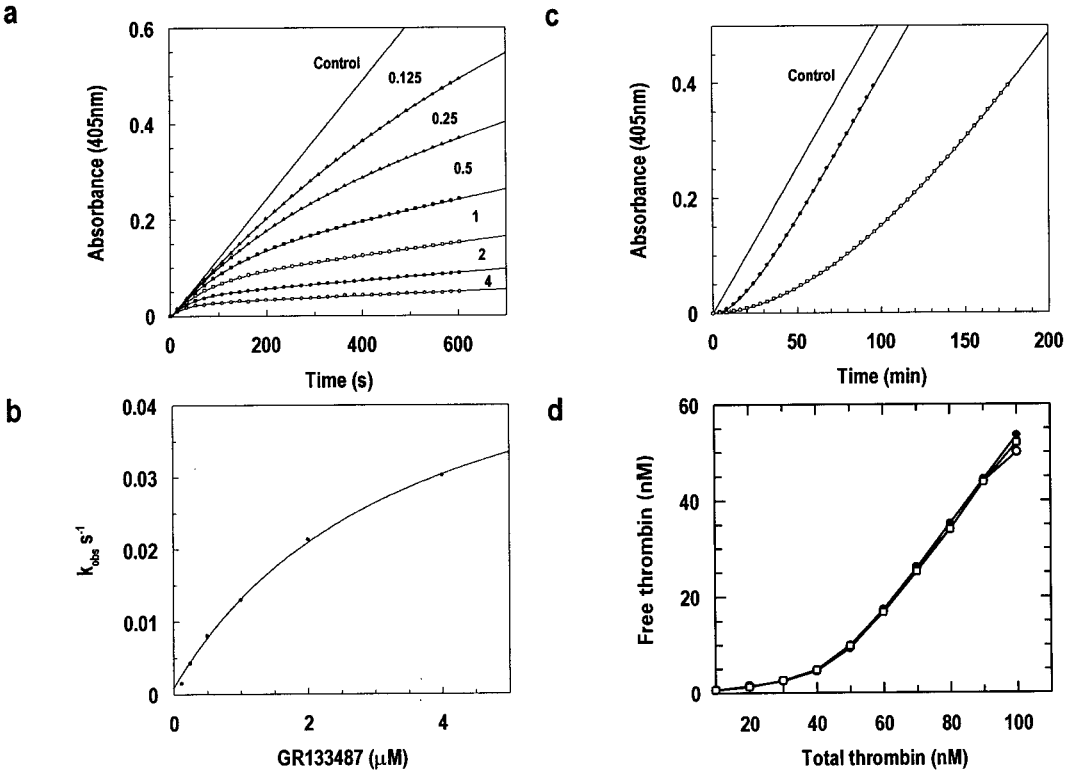

FIGURE 3: (a) Progress curves of slow-binding α-thrombin inhibition by GR133487 at pH 8.4. Reactions were initiated by addition of inhibitor and substrate, 990 μL, to enzyme solution, 10 μL, in 50 mM Tris-HC1 buffer containing 0.5 M NaCl and 0.1% PEG 6000. Final inhibitor concentrations for each curve were as labeled, and final enzyme concentration was 1 nM. Except at higher inhibitor concentrations (micromolar), initial rates of substrate hydrolysis were similar to rates with uninhibited enzyme (control). Solid lines are the integrated rate equation (eq 3) fitted to the data of each curve from which the pseudo-first-order rate constant for inhibition, k_{obs}, is derived. (b) Replot of k_{obs} versus [I] for inhibition of α-thrombin by GR133487 at pH 8.4. k_{obs} approaches a limit at higher concentrations of GR133487, indicating saturation of the enzyme. The solid line is eq 2 fitted to the data, taking into account the predetermined value of k_4. Similar plots were obtained for GR133487 and GR133686 at pH 6.0. For GR133686 at pH 8.4, the relationship between k_{obs} and [I] was linear and was analyzed by fitting eq 1 to the data. (c) Progress curves of dissociation of α-thrombin activity from preformed inhibited complexes with GR133487 (●) and GR133686 (□) at pH 8.4. Buffer conditions were as in panel a. For conditions see main text. Solid lines are eq 3 fitted to the data of each curve. (d) Residual α-thrombin activity in enzyme−inhibitor complexes with GR133487 at pH 8.4. α-Thrombin at the final concentrations indicated was mixed with GR133487 at a final concentration of 50 nM. Plots of residual activity determined at 30 (○), 90 (●) and 180 min (□) after mixing are superimposable, indicating minimal breakdown of the inhibitor.

Table 3: Summary of α-Thrombin Inhibition Kinetic Data for GR133487 and GR133686 and Some Comparative Inhibition Data (*49*−*55*)

	k_{on} (s^{-1} M^{-1})	k_4 or k_{off} (s^{-1})	K_i	k_3 (s^{-1})	K_i*	$t_{1/2}$[a] (min)
GR133487,[b] pH 8.4	1.71×10^6	8.4×10^{-4}	24 nM	0.041	480 pM	13.75
GR133487,[b] pH 6.0	0.037×10^6	1.3×10^{-4}	0.97 μM	0.036	3.5 nM	89
GR133686,[c] pH 8.4	4.6×10^6	1.3×10^{-4}	28 pM			89
GR133686,[b] pH 6.0	0.296×10^6	7.1×10^{-6}	0.83 μM	0.246	24 pM	1620
antithrombin III	7.4×10^3	2.6×10^{-6}	1.4 mM	10.4	310 pM	4442
heparin−antithrombin III	1.4×10^6	2.3×10^{-6}	4.0 μM	5.4		5021
protease nexin 1	1.8×10^6	1.7×10^{-5}	3.4 μM	6.0	11 pM	679
PPACK	1.2×10^7	na	0.13 μM	125	na	na
Eoc-Phe-Pro-azaLys-p-Np	$>1.6 \times 10^7$		<500 nM	8.0		
Boc-(D)Phe-Pro-boroArg-OH	9.3×10^6	1.7×10^{-5}	720 pM	0.007	3.6 pM	679
fluorescein mono-*p*-guanidinobenzoate hydrochloride	2.77×10^3	1.78×10^{-3}	22 μM	0.06	630 nM	6.49
4-chloro-7-guanidino-3-methoxyisocoumarin	2.9×10^5		10 nM	0.003		

[a] Calculated from the relationship $t_{1/2} = 0.693/k_4$. [b] Analyzed according to Scheme 2 and eq 2. k_{on} is the apparent second-order rate constant for inhibition, k_3/K_i; K_i* is the overall dissociation constant for a slow-binding inhibition mechanism and is calculated as $K_i^* = K_i k_4/(k_3 + k_4)$ (*38*). [c] Analyzed according to Scheme 1 and eq 1.

inactivated (<5% residual activity compared to control enzyme). Figure 3c illustrates the recovery of α-thrombin activity from a complex of thrombin and GR133487 at pH 8.4. k_{dis} was measured over a range of inhibitor concentrations (2.5−40 μM) and was found to be identical, confirming that dilution was sufficient to make inhibition negligible under steady-state conditions and that k_{dis} is equivalent to k_{off} or k_4. Using the values of k_4 derived from dissociation progress curves, plots of k_{obs} versus [I] as shown in Figure 3b were fitted to eq 2 and used to derive estimates of k_3 and K_i. k_{off} values for GR133686 at pH 8.4 allowed estimation of k_{on} (eq 1) from progress curve data. These data are summarized in Table 3, along with literature values of other thrombin inhibitors for comparison.

The kinetic and structural observations led to speculation that the tight complex inferred from progress curves was the

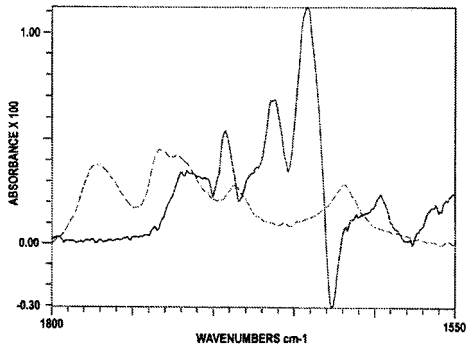

FIGURE 4: FT-IR difference spectrum of GR133686 complexed to α-chymotrypsin minus free chymotrypsin (solid line) at pH 7.4 superimposed upon the spectrum of free GR133686 in 40% acetonitrile/60% D_2O (dashed line). The band at 1766 cm^{-1} in free GR133686 is due to the *trans*-lactone carbonyl; its disappearance on complex formation is attributed to acylation of the enzyme (see text) where it would contribute to the ester carbonyl band at 1714 cm^{-1}.

product of acylation of the Ser195 due to attack on the *trans*-lactone carbonyl and that k_4 or k_{off} represented the deacylation rate constant. According to Schemes 1 or 2, the deacylation step would re-form the intact inhibitor by relactonization. However, it was also possible that slow turnover of inhibitor was occurring and the inhibitors were acting as alternate substrates (*38*). To test the relevance of this mechanism to the inhibition of α-thrombin by GR133487 and GR133686, residual activity of near-stoichiometric mixtures was assayed during prolonged incubation. For 2.5 μM GR133487 at a 1.25 molar excess to enzyme (pH 8.4), residual activity was stable at 3−4% of control enzyme activity for at least 180 min; for GR133686 at pH 8.4 at a 2.5-fold molar excess of inhibitor, residual activity again was stable at less than 1% of control enzyme activity to 240 min of incubation. At 60 min intervals over 4 h, samples were removed for dissociation progress curves, which showed that for both inhibitors the k_4 value and final steady-state activity were constant over this period. These results argue against the occurrence of inhibitor hydrolysis. A more detailed study of α-thrombin inhibition by GR133487 at pH 8.4 is shown in Figure 3d; 50 nM GR133487 was mixed with α-thrombin over a range of concentrations from inhibitor excess to enzyme excess. Those combinations at which α-thrombin is in excess (>50 nM) are essentially under single-turnover conditions, in that if turnover was occurring, the EI* complex would decay in a first-order manner and enzymatic activity should be regained at a rate consistent with a half-time of the inhibited complex of 13.75 min (0.693/k_4); plots at 30, 90, and 180 min are superimposable, confirming the low or absent rate of turnover.

Fourier Transform Infrared. Initial evidence of breakage of the lactone ring and putative serine acylation came from FT-IR studies of the α-chymotrypsin/GR133686 complex. As shown in Figure 4, GR133686 exhibits a strong lactone carbonyl band at 1766 cm^{-1} in 40% CH_3CN/60%D_2O and a broader band at 1718 cm^{-1} corresponding to the ester carbonyls. Difference spectra were obtained by subtracting the spectrum of free α-chymotrypsin from the α-chymotrypsin/GR133686 complex and show a broad band at 1714 cm^{-1} specific for the compound and presumed acyl-enzyme ester carbonyls, plus peaks in the protein amide I band due to ligand-induced perturbations to the enzyme (*45*); the absence

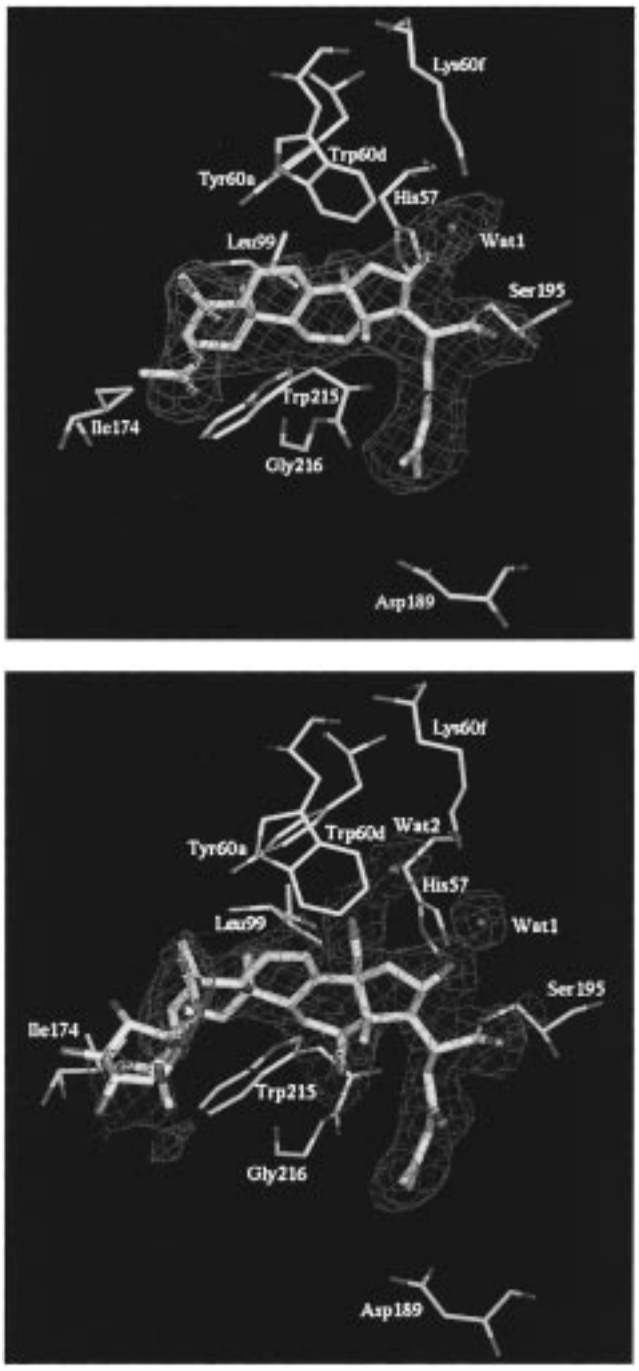

FIGURE 5: Difference electron density maps contoured at 2σ for (a, top) GR133686 and (b, bottom) GR133487 bound to the α-thrombin active site. The density in both cases shows a ring-opened conformation of the inhibitor and a covalent bond to Ser195. Electron density features close to the NZ atom of Lys60f have been interpreted as water molecules (see text).

of a *trans*-lactone peak at higher wavenumbers is consistent with ring opening and acylation, since the required shift of over 40 cm^{-1} cannot realistically be explained by hydrogen bonding alone and is consistent with a mode of binding in which the ester carbonyl is hydrogen-bonded in the oxyanion hole (*45*).

Further evidence in α-thrombin for acyl-enzyme adduct formation was obtained by protein crystallographic and mass spectrometry studies outlined below.

X-ray Crystallography. X-ray crystallographic studies were employed in order to identify the molecular details of

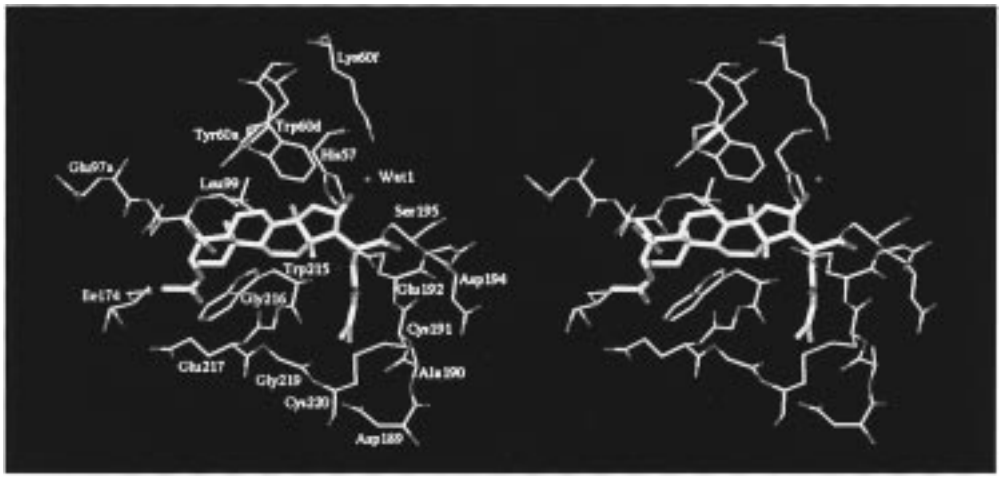

FIGURE 6: Stereoview of the α-thrombin active site showing key residues that interact with GR133686; the inhibitor is shown with thicker bonds. The inhibitor hydroxyl of the ring-opened lactone hydrogen bonds to Lys60f via a water molecule (Wat1). The neutral enone inhibitor side chain occupies the S1 pocket, largely by hydrophobic interactions; its carbonyl oxygen does not appear to be hydrogen-bonded. S2 is only partially occupied and S3 is unoccupied.

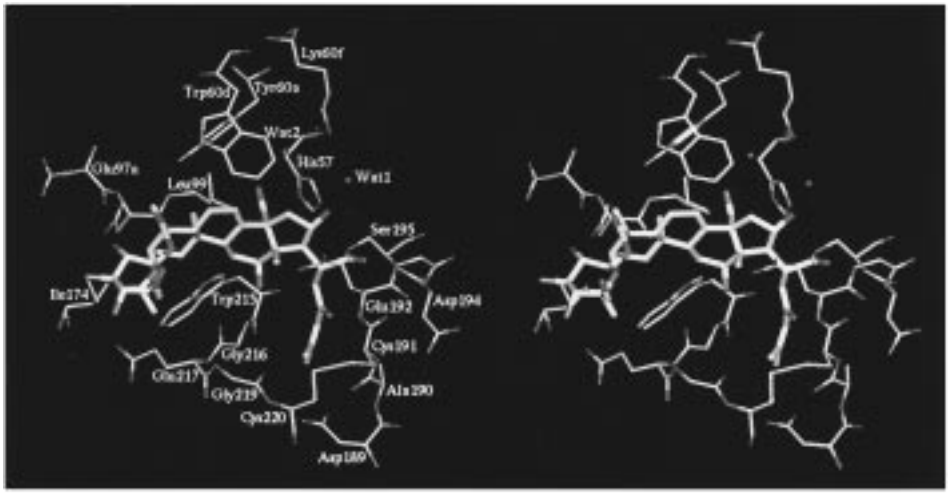

FIGURE 7: Stereoview of active-site-bound GR133487 showing the primary interactions with key residues. As for GR133686, the hydroxyl interacts with Lys60f via Wat1, but the additional hydroxymethyl group of GR133487 results in a second bridging water molecule to Lys60f; this water is located in the S2 pocket (Wat2). The glycoside and ester groups protrude into solvent. In all other respects the inhibitor conformations are indistinguishable within experimental error.

the binding modes of GR133686 and GR133487 to human α-thrombin. The structure of the α-thrombin/GR133686 complex was solved to 3 Å resolution and shows the inhibitor at the active site in a ring-opened conformation (Figure 5a). Moreover, electron density around the Ser195 is consistent with a covalent bond between the protein and inhibitor. The S1 pocket of the enzyme is occupied by the enone side chain, which makes mostly van der Waals interactions. The enone carbonyl makes no hydrogen bonds to the protein, and due to the hydrophobic nature of the side chain there is no interaction with Asp189 at the bottom of the S1 pocket (Figure 6). A prominent hydrogen-bonding network is observed between the inhibitor hydroxyl, a water molecule, and NZ of Lys60f. The presence of electron density for this water molecule in both molecules of the asymmetric unit reinforces this interpretation even at this medium resolution. Another hydrogen-bonding pattern is observed in the oxyanion hole (*46*); the inhibitor carbonyl oxygen hydrogen-bonds to 193NH (2.6 Å) and 195NH (2.7 Å), although this latter hydrogen bond is not of optimal geometry. This observation is consistent with the FT-IR results presented above for the α-chymotrypsin complex in free solution. The remaining protein/inhibitor interactions are largely van der Waals with partial occupation of the S2 pocket by an equatorial methyl group; the S3 pocket as defined by Leu99, Ile174 and Trp215 remains unoccupied. The methyl ester and the carboxylic groups protrude into solvent.

X-ray analysis of the α-thrombin/GR133487 complex at 2.2 Å resolution defined, in general, a similar binding mode (Figures 5b and 7). Thus, the inhibitor is in the ring-opened conformation and a covalent bond between Ser195 and the lactone carbonyl is formed. A similar network of hydrogen bonds is observed between the inhibitor hydroxyl and Lys60f via a water molecule as well as the oxyanion hole interactions; the inhibitor carbonyl oxygen is hydrogen-bonded to 193NH (2.8 Å) and 195NH (2.9 Å). The enone side chain occupies the S1 pocket in a manner similar to the α-thrombin/GR133686 complex. There are several differences between the structures of GR133686 and GR133487, one of which is that GR133487 has a hydroxymethyl group instead of a methyl on ring C of the triterpene structure (Figure 1). This hydroxymethyl group results in greater occupation of the S2

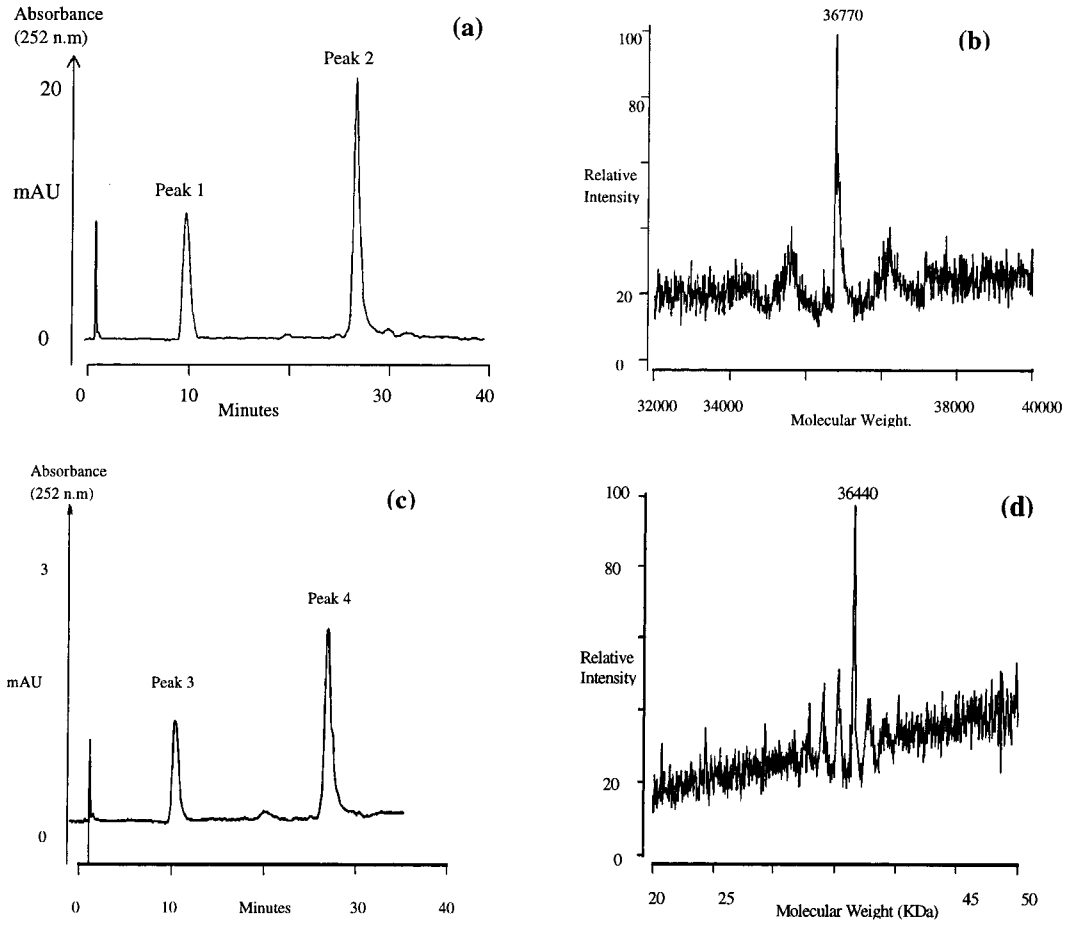

FIGURE 8: (a) RP-HPLC separation of α-thrombin incubated for 5 min with a 5-fold molar excess of GR133487. Spiking with standards gave a retention time of 10 min for GR133487, 27 min for α-thrombin, and 8 min for the synthetic ring-opened hydrolysis product of the *trans*-lactone. Components 1 and 2 were collected, dried under vacuum, redissolved, and analyzed by ESI-MS. (b) Molecular mass of component collected in peak 2, obtained from computer deconvolution of the ESI-MS mass spectrum rounded to the nearest 10 mass units. (c) RP-HPLC separation of mixture of PPACK added to preformed α-thrombin/GR133487 complex and incubated for 60 min. Peak 3 was confirmed as free intact GR133487 by ESI-MS. (d) ESI-MS of peak 4. The molecular ion corresponds to the α-thrombin/PPACK adduct, which is formed quantitatively.

pocket and allows a water molecule (Wat 2) to bind in this hydrophobic pocket by providing hydrogen-bonding potential. This water molecule participates in a network of hydrogen bonds as it is positioned 2.9 Å from the hydroxymethyl oxygen and also 2.9 Å from the NZ of Lyz60f, which results in Lys60f being solvated by two water molecules in the α-thrombin/GR133487 complex as opposed to only one water in the α-thrombin/GR133686 complex. A further difference between the two inhibitors is the presence of a hydroxyl substituent on the C ring of the GR133487. This hydroxyl oxygen atom hydrogen-bonds to the amide nitrogen of Gly216 (3.2 Å); furthermore, the hydroxyl proton may also hydrogen-bond to the carbonyl of Gly216, as the heavy atom distance is 3.2 Å. The glycoside and ester moieties of GR133487 make little contact with the protein and protrude into solvent.

Demonstration of Reversible Acylation of α-Thrombin by GR133487 by RP-HPLC and Mass Spectrometry. Given the propensity for acyl-enzyme formation shown crystallographically for α-thrombin/GR133686 and α-thrombin/GR133487 and by FT-IR for α-chymotrypsin/GR133686, it can be inferred that the tightly bound complex EI* is the acyl-enzyme. The reversibility seen in the kinetic data can therefore be explained by relactonization, with release of intact inhibitor. Proof of this mechanism requires (a) demonstration that the predominant species in the presence of excess inhibitor is the acyl-enzyme and (b) direct evidence of *trans*-lactone release from this acyl-enzyme. Formation of a covalent adduct with α-thrombin was demonstrated by RP-HPLC and ESI-MS. GR133487 was added in 5-fold excess over human α-thrombin at pH 6.0; the mixture was then separated by RP-HPLC (Figure 8a) and the resultant peaks were analyzed by ESI-MS. Peak 1 had $m/z = 735.3$, equivalent to the protonated molecular ion for the intact *trans*-lactone form of GR133487. Peak 2, $m/z = 36\,770$, is equivalent to the α-thrombin/GR133487 complex (Figure 8b). This complex is almost certainly covalent and therefore equivalent to the acyl-enzyme seen in the crystal structure, as the observation of noncovalent binding by ESI-MS requires milder conditions than employed here (*47*). Free α-thrombin coelutes with α-thrombin complex, but its $m/z = 36\,030$, a mass shift of approximately 740 corresponding to acylation by the inhibitor. No hydrolyzed GR133487 (hydroxy acid) was observed by RP-HPLC after 3 h of incubation, confirming that enzyme-catalyzed turnover of this inhibitor is negligible. In addition, denaturation of the α-thrombin/GR133487 complex in 6 M guanidine hydrochloride prior to ESI-MS did not cause dissociation. Finally, the autolytically "nicked" fragment, residues 155−259 (*48*), was observed by ESI-MS to shift from $m/z = 11\,947$ to m/z

= 12 683 (plus GR133487) and to m/z = 12 489 (plus GR133686); this fragment contains the active-site serine isolated from the other members of the catalytic triad, confirming formation of a covalent adduct.

Under the relatively high enzyme and inhibitor concentrations (micromolar) employed for the mass spectrometry experiments, the equilibrium concentration of free inhibitor is expected to be very low, making direct observation of regenerated *trans*-lactone problematic. Instead, we attempted to perturb the equilibrium by the addition of the irreversible α-thrombin inhibitor PPACK (*20*); formation of the α-thrombin/PPACK adduct should displace the equilibrium shown in Schemes 1 and 2 at a rate governed by the slow deacylation rate, k_4 or k_{off}, with concomitant buildup of free *trans*-lactone. Acylated α-thrombin was formed by addition of 5-fold excess of GR133487 and then free inhibitor separated from the acyl-enzyme by membrane filtration; no free inhibitor was detectable by RP-HPLC. One equivalent of PPACK was then added to the complex and incubated for 60 min and the mixture was analyzed by RP-HPLC and ESI-MS (Figure 8c). The α-thrombin HPLC peak (peak 4) had m/z = 36 440, equivalent to the PPACK adduct; no molecular ion corresponding to α-thrombin/GR133487 was observed (Figure 8d). An additional peak (peak 3) was observed at the same retention time as authentic GR133487 (Figure 8c); ESI-MS showed a molecular ion m/z = 735, corresponding to GR133487, plus a major fragment ion at m/z 573 due to loss of the hexose, confirming the assignment. Peak 3 could be eliminated by further addition of excess thrombin to the mixture; subsequent ESI-MS analysis of peak 4 showed the presence of free enzyme, α-thrombin/PPACK, and α-thrombin/GR133487 adducts, indicating that reversible release of reactive GR133487 from the acyl-enzyme had occurred upon addition of PPACK.

It could be argued, although mechanistically it appears unlikely, that PPACK acts directly on the acyl-enzyme to displace the *trans*-lactone rather than reacting with free enzyme; if so, then the more slowly deacylating inhibitor GR133686, whose half-life complexed to α-thrombin at pH 6.0 is 18-fold longer that of GR133487 (Table 3), should also be rapidly displaced from its acyl-enzyme. However, 3 h of incubation of PPACK at pH 6.0 with α-thrombin/GR133686 produced only a peak corresponding to the GR133686 adduct (m/z = 36 570) with no detectable displaced GR133686 or α-thrombin/PPACK complex, consistent with the assumption that formation of this adduct is governed by k_4.

Taken together, the kinetic, crystallographic, and spectroscopic data best describe GR133487 and GR133686 as tight-binding reversible inhibitors of α-thrombin that act by acylation of the active-site serine, with the deacylation (ring closure) rate being approximately 6−18 times greater for GR133487.

DISCUSSION

The *trans*-lactone compounds presented here represent a novel class of competitive reversible α-thrombin inhibitors that form a stable acyl-enzyme intermediate. These compounds are extremely potent inhibitors of thrombin, with apparent second-order inhibition rate constants in excess of 10^6 s^{-1} M^{-1}. The high level of stability and therefore potency is in part due to strong noncovalent binding, as shown by submicromolar K_i values (Table 3) and partial burial of the hydrophobic inhibitor framework in the active site (Figures 6 and 7), and in part due to acylation driven by the strained *trans*-lactone ring combined with the observed hydrolytic stability of the acyl-enzyme. These association rate constants listed in Table 3 compare favorably with other potent two-step thrombin inhibitors reported in the literature (*49*−*55*), some of which are listed for comparison. For example, the association rate constants at pH 8.4 are within an order of magnitude of those reported for the most potent peptidyl inhibitors of thrombin PPACK (chloromethyl ketone) (*20, 52*), Eoc-Phe-Pro-azaLys-p-Np (acylating active-site titrant) (*53*), and H-D-Phe-Pro-boroArg-OH (slow-binding reaction intermediate analogue) (*54*) and are directly comparable to rates of inhibition for heparin-catalyzed antithrombin III (*49*) and for the serpin protease nexin 1 (*51*). It can be seen from the table that the most potent thrombin inhibitors (apparent second-order rate constants greater than 10^6 s^{-1} M^{-1}) are generated by initial K_i values in the range 2.8×10^{-11} to 4.0×10^{-6} M and rate constants for conversion to the final complex (k_3) in the range 0.007−125 s^{-1}. With a rate constant for the conversion of the noncovalent complex at the lower end of the range, the remarkable second-order inhibition constants for the compounds described here are largely the result of good recognition for the active site of thrombin. These natural product inhibitors of thrombin are therefore comparable to or better than the most tight-binding synthetic nonpeptide inhibitor we are aware of, 4-chloro-7-guanidino-3-methoxyisocoumarin (Table 3; *15*).

The substantial reduction in k_4 or k_{off} at pH 6.0 compared to pH 8.4 is consistent with the expected effect of His57 ionization on the deacylation rate (*56*) and therefore with the proposed mode of action of the inhibitors. On the basis of IC_{50} measurements against other serine proteases, the inhibitors GR133487 and GR133686 exhibit limited specificity for α-thrombin (Table 2). This is explained in part by the crystal structures of the acyl complexes, which show that the neutral enone side chain occupying S1 appears to lack hydrogen-bonded interactions with the protein and so may not discriminate at this position against other enzymes such as α-chymotrypsin, which also possesses a deep S1 pocket (*44*); in contrast, inhibition is negligible against factor Xa and XIIa and weak against factor XIa, plasmin, tPA, and cathepsin G, which accept Arg, Lys, or Phe in their S1 pockets, suggesting the remainder of the inhibitor binds less well to these enzymes. It is also noteworthy that α-thrombin inhibitors usually require a positively charged group occupying S1, and there is only one other reported three-dimensional structure of an α-thrombin/inhibitor complex with a neutral S1 group (*57*).

The *trans*-lactone inhibition mechanism is unusual in that most heterocyclic inhibitors of serine proteases show deacylation by hydrolysis rather than recyclization, and in the case of mechanism-based inhibitors show partitioning between inactivated species, stable acyl-enzymes, or hydrolytic products (*10, 11, 58*). For example, the ynenol lactone (*18*), 3-benzyl-6-chloro-2-pyrone (*16*), isatoic anhydride (*19*), enol lactone (*17, 59*), 3-alkoxy-4-chloroisocoumarin (*15, 60, 61*), benzisothiazolone (*62, 63*) and β-lactam (*12*−*14*) series of inhibitors are not reported to show recyclization as a

significant mode of deacylation, even though stable acyl-enzymes are formed in some cases and reversal must be possible. Equilibration between acyl-enzyme and parent heterocycle has been reported, however, for 2-methyl-4*H*-3,1-benzoxazin-4-one-inhibited α-chymotrypsin (*64*) and can be a dominant deacylation pathway for some elastase inhibitors of this class (*65, 66*). Recyclization of simple nitrobenzyl lactone and phosphate ester adducts of α-chymotrypsin was also observed by Kaiser (*67*). The photoisomerization and lactonization of enzyme-bound cinnamoyl esters to form coumarin products (*68, 69*) is also analogous.

To understand the cause of the high hydrolytic stability of the GR133487 and GR133686 α-thrombin acyl-enzymes, factors controlling the deacylation rate need to be considered. There are several ways in which this rate can be reduced, for example, by rotation of His57 following acylation into a catalytically inactive "out" position as seen in some elastase and trypsin inhibitor complexes (*70, 71*), lack of oxyanion hole occupancy by the ester carbonyl (*70*−*72*), or suboptimal stereoelectronic alignment of the ester due to poor subsite occupancy (*56*). Steric or electrostatic repulsion or deactivation of water has indeed been exploited in the design of deacylation-stable benzoxazinones (*65*) and a penicillanate *β*-lactamase inhibitor that was made stable to deacylation by displacement or hydrogen bonding of the hydrolytic water molecule (*73*). Furthermore, an inhibitor carboxylate observed to form a salt bridge to His57 in 3-benzyl-6-chloropyrone-inactivated chymotrypsin was proposed to stabilize the complex by exclusion of hydrolytic water (*74*).

Examination of the α-thrombin/inhibitor X-ray structures presented here offers an understanding of their hydrolytic stability. In both acyl-enzymes the catalytic triad appears to be undisrupted, and the oxyanion hole is occupied by the ester carbonyl, suggesting these factors are not the cause of impaired hydrolysis. However, in both complexes the inhibitor hydroxyl occupies the space between His57 and the ester carbonyl that might otherwise be taken by a deacylating water molecule; the hydroxyls appear to be held firmly in place due to good complementary interactions with the active site and the rigidity of the inhibitor backbone, so there is little likelihood of displacement by extraneous solvent, suggesting water expulsion is the reason for the lack of deacylation. The high resolution of the α-thrombin/GR133487 complex structure allows this hypothesis to be examined in some detail. The distance between the GR133487 hydroxyl and Nϵ of His57 is 2.9 Å, and the angle between the plane of the imidazole and the hydroxyl oxygen is 157°; the distance and angle of the hydroxyl oxygen and ester carbonyl carbon are 3.0 Å and 100°. Similar interactions are observed in α-thrombin/GR133686, although the lower resolution of this structure precludes precise comparison. This geometry is suitable for base-catalyzed nucleophilic attack (*75*) and places the hydroxyl in an analogous position to the water for substrate deacylation recently proposed by Wilmouth et al. (*2*) for a porcine pancreatic elastase/peptide acyl-enzyme. Other deacylating water molecules have also been proposed, one of which is conserved in a number of serine proteases and hydrogen bonds to the carbonyl of residue Leu41 (chymotrypsin numbering; *76*) and is indeed observed here in the α-thrombin/GR133487 structure; however, this water would need to move into the position blocked by the inhibitor hydroxyl to enable base-catalyzed attack on the ester. Singer et al. (*77*) showed the appearance of a water molecule above the P1 pocket by time-resolved Laue crystallography of trypsin-catalyzed hydrolysis of a *p*-guanidinobenzoate intermediate; this region is occluded by the five-membered ring of the inhibitor in our structures and would also be blocked by peptide substrates. These results suggest that the water observed by Wilmouth et al. is the most likely candidate molecule for peptide substrate deacylation, and therefore that α-thrombin/GR133487 relactonization may be an interesting model for this reaction.

The question then arises as to why deacylation by ring closure is an order of magnitude faster for GR133487? This is unclear, although the following observations may be significant: the hydroxyl of GR133686 forms a water-mediated hydrogen bond to the positively charged side-chain amino group of Lys60f (Figure 6), with an inhibitor hydroxyl oxygen/NZ heavy atom distance of 3.7 Å (4.4 Å for the second molecule in the asymmetric unit); in the case of GR133487 a hydroxymethyl group (rather than methyl for GR133686) in the hydrophobic S2 pocket draws in an additional water molecule hydrogen-bonded to Lys60f (Figure 7), and also the Lys60f NZ/inhibitor hydroxyl distance in the GR133487 complex is increased to 5 Å; it is possible that this water-mediated interaction of Lys60f and the nucleophilic hydroxyl causes a reduction in reactivity and therefore a stabilization of the acyl-enzyme, an effect that would be lessened in GR133487 by greater distance and screening by the second water molecule. Clearly, though, at this resolution and given the subtlety of mechanistic effects, it is impossible to be sure of the reasons for this difference.

In conclusion, a combination of proflavin displacement, kinetic analysis, FT-IR, mass spectrometry, and protein X-ray crystallography have shown that the novel natural product inhibitors GR133686 and GR133487 inhibit α-thrombin, α-chymotrypsin, and probably other serine proteases due to acylation by their 5,5-*trans*-lactone moieties and that at least in the case of α-thrombin this inhibition is reversible, with regeneration of lactone rather than hydrolysis as the mode of dissociation. The inhibitor hydroxyl that attacks the seryl ester to effect relactonization may well occupy the position normally taken by water during deacylation of peptide substrates and could be considered a model for this reaction. This information forms the basis for exploitation of this new class of serine protease inhibitors in drug discovery.

ACKNOWLEDGMENT

We thank Vivienne Urquhart for help in preparation of the manuscript; Anil Mistry for assistance in crystallization; Terry Haley for his contribution to the mass spectrometry studies; Sara Witham and Champa Patel for their assistance on kinetic studies; Mary Noble and John Farthing for supply of materials; Andrew White, University of Staffordshire, for FT-IR studies; and Mike Hann, Nigel Watson, and Robert Cooke for helpful comments.

REFERENCES

1. O'Neill, M. J., Lewis, J. A., Noble, H. M., Holland, S., Mansat, C., Farthing, J. E., Foster, G., Noble, D., Lane, S. J., Sidebottom, P. J., Lynn, S., Hayes, M. V., and Dix, C. J. (1998) *J. Nat. Prod.* (submitted for publication).

2. Wilmouth, R. C., Clifton, I. J., Robinson, C. V., Roach, P. L., Aplin, R. T., Westwood, N. J., Hajdu, J., and Schofield, C. J. (1997) *Nat. Struct. Biol. 4* (8), 456−462.
3. Davie, E. W., Fujikawa K., and Kisiel, W. (1991) *Biochemistry 30*, 10363−10370.
4. Esmon, C. T. (1995) *FASEB J. 9*, 946−955.
5. Vu, T.-K. H., Hung, D. T., Wheaton, V. I., and Coughlin, S. R. (1991) *Cell 64*, 1057−1068.
6. Stubbs, M. T., and Bode, W. (1993) *Thromb. Res. 69*, 1−58.
7. Skrzypczak-Jankun, E., Carperos, V. E., Ravichandran, K. G., Tulinsky, A., Westbrook, M., and Maraganore, J. M. (1991) *J. Mol. Biol. 221*, 1379−1393.
8. Schechter, I., and Berger, A. (1967) *Biochem. Biophys. Res. Commun. 27*, 157−162.
9. Bode, W., Mayr, I., Baumann, U., Huber, R., Stone, S. R., and Hofsteenge, J. (1989) *EMBO J. 8*, 3467−3475.
10. Powers, J. C., and Harper, J. W. (1986) in *Proteinase Inhibitors* (Barrett, A. J., and Salvesen, G., Eds.) pp 55−152, Elsevier, Amsterdam.
11. Wharton, C. W. (1997) in *Comprehensive Biological Catalysis* (Sinnott, M., Ed.) Vol. 1, Chapter 11, Academic Press, London.
12. Navia, M. A., Springer, J. P., Lin, T. Y., Williams, H. R., Firestone, R. A., Pisano, J. M., Doherty, J. B., Finke, P. E., and Hoogsteen, K. (1987) *Nature 327*, 79−82.
13. Knight, W. B., Maycock, A. L., Green, B. G., Ashe, B. M., Gale, P., Weston, H., Finke, P. E., Hagmann, W. K., Shah, S. K., and Doherty, J. B. (1992) *J. Am. Chem. Soc. 31*, 4980−4986.
14. Underwood, D. J., Green, B. G., Chabin, R., Mills, S., Doherty, J. B., Finke, P. E., MacCoss, M., Shah, S. K., Burgey, C. S., Dickinson, T. A., Griffin, P. R., Lee, T. E., Swiderek, K. M., Covey, T., Westler, W. M., and Knight, W. B. (1995) *Biochemistry 34*, 14344−14355.
15. Kam, C.-M., Fujikawa, K., and Powers, J. C. (1988) *Biochemistry 27*, 2547−2557.
16. Gelb, M. H., and Abeles, R. H. (1984) *Biochemistry 23*, 6569−6604.
17. Katzenellenbogen, J. A., Rai, R., and Dai, W. (1992) *Bioorg. Med. Chem. Lett. 2* (11), 1399−1404.
18. Copp, L. J., Krantz, A., and Spencer, R. W. (1987) *Biochemistry 26*, 169−178.
19. Gelb, M. H., and Abeles, R. H. (1986) *J. Med. Chem. 29*, 585−589.
20. Kettner, C., and Shaw, E. (1979) *Thromb. Res. 14*, 969−973.
21. Bone, R., Shenvi, A. B., Kettner, C. A., and Agard, D. A. (1987) *Biochemistry 26*, 7609−7614.
22. Brady, K., Wei, A., Ringe, D., and Abeles, R. H. (1990), *Biochemistry 29*, 7600−7607.
23. Gorenstein, D. G., and Shah, D. O. (1982) *Biochemistry 21*, 4679−4686.
24. Tapparelli, C., Metternich, R., Ehrhardt, C., Zurini, M., Claeson, G., Scully, M. F., and Stone, S. R. (1993) *J. Biol. Chem. 268*, 4734−4741.
25. Turpie, A. G., Weitz, J. I., and Hirsh., J. (1995) *Thromb. Haemostasis 74*, 565−571.
26. Callas, D., and Fareed, J. (1995) *Thromb. Haemostasis 74*, 473−481.
27. Engh, R. A., Brandstetter, H., Sucher, G., Eichinger, A., Baumann, U., Bode, W., Huber, R., Poll, T., Rudolph, R., and von der Saal, W. (1996) *Structure 4*, 1353−1360.
28. Fenton, J. W., Fasco, M. J., and Stackrow, A. B. (1977) *J. Biol. Chem. 252*, 3587−3598.
29. Ngai, P. K., and Chang, J.-Y. (1991) *Biochem. J. 280*, 805−808.
30. Lottenberg, R., Christensen, U., Jackson, C. M., and Coleman, P. L. (1981) *Methods Enzymol. 80*, 341−361.
31. Berliner, L. J, and Shen, Y. Y. L. (1977) *Biochemistry 16*, 4622−4626.
32. Schonbaum, G. R., Zerner, B., and Bender, M. L. (1961) *J. Biol. Chem. 236*, 2930−2935.
33. Lottenberg, R., Hall, J. A., Fenton., J. W., II., and Jackson, C. M. (1982) *Thromb. Res. 28*, 313−332.
34. Chmielewska, J., Ranby, M., and Wiman, B. (1988) *Biochem. J. 251*, 327−332.
35. Lottenberg, R., Hall, J. A., Pautler, E., Zupan, A., Christensen, U., and Jackson, C. M. (1986) *Biochim. Biophys. Acta 874*, 326−336.
36. Nakajima, K., Powers, J. C., Ashe, B. M., and Zimmerman, M. (1979) *J. Biol. Chem. 254*, 4027−4032.
37. Hoylaerts, M., Rijken, D. C., Lijnen, H. R., and Collen, D. (1982) *J. Biol. Chem. 257* (6), 2912−2919.
38. Morrison, J. F., and Walsh, C. T. (1988) *Adv. Enzymol. Relat. Areas Mol. Biol. 61*, 201−301.
39. McPherson, A. (1992) *J. Cryst. Growth 122*, 161−167.
40. Messerschmidt, A., and Pflugrath, J. W. (1987) *J. Appl. Crystallogr. 20*, 306−315.
41. Brünger, A. T., Kuriyan, J., and Karplus, M. (1987) *Science 235*, 458−460.
42. Himoe, A., Brandt, K. G., DeSa, R. J., and Hess, G. P. (1969) *J. Biol. Chem. 244*, 3483−3493.
43. Sonder, S. A., and Fenton, J. W., II (1984) *Biochemistry 23*, 1818−1823.
44. Perona, J. J., and Craik, C. S. (1995) *Protein Sci. 4*, 337−360.
45. White, A. J., and Wharton, C. W. (1990) *Biochem. J. 270*, 627−637.
46. Bode, W., Turk, D., and Karshikov, A. (1992) *Protein Sci. 1*, 426−471.
47. Ganem, B., Li, Y.-T., and Henion, J. D. (1991) *J. Am. Chem. Soc. 113*, 6294−6296.
48. Guillin, M. C., and Bezeaud, A. (1992) *Semin. Thromb. Haemostasis 18*, 224−229.
49. Olson, S. T., and Shore, J. D. (1982) *J. Biol. Chem. 24*, 14891−14895.
50. Danielsson, A., and Bjork, I. (1983) *Biochem. J. 213*, 345−353.
51. Stone, S. R., and Hermans, J. M. (1995) *Biochemistry 34*, 5164−5172.
52. Lijnen, H. R., Uytterhoeven, M., and Collen, D. (1984) *Thromb. Res. 34*, 431−437.
53. De Simone, G., Balliano, G., Milla, P., Gallina, C., Giordano, C., Tarricone, C., Rizzi, M., Bolognesi, M., and Ascenzi, P. (1997) *J. Mol. Biol. 269*, 558−569.
54. Kettner, C., Mersinger, L., and Knabb, R. (1990) *J. Biol. Chem. 265*, 18289−18297.
55. Melhado, L. L., Peltz, S. W., Leytus, S. P., and Mangel, W. F. (1982) *J. Am. Chem. Soc. 104*, 7299−7306.
56. Fersht, A. R. (1985) *Enzyme Structure and Mechanism*, W. H. Freeman and Co., New York.
57. Malikayil, J. A., Burkhart, J. P, Schreuder, H. A., Broersma, R. J., Jr., Tardif, C., Kutcher, L. W., III, Mehdi, S., Schatzman, G. L., Neises, B., and Peet, N. P. (1997), *Biochemistry 36*, 1034−1039.
58. Edwards, P. D., and Bernstein, P. R. (1994) *Med. Res. Rev. 14*, 127−194.
59. Baek, D.-J., Reed, P. E., Daniels, S. B., and Katzenellenbogen, J. A. (1990) *Biochemistry 29*, 4305−4311.
60. Harper, J. W., and Powers, J. C. (1985) *Biochemistry 24*, 7200−7213.
61. Kerrigan, J. E., Oleksyszyn, J., Kam, C.-M., Selzler, J., and Powers, J. C. (1995) *J. Med. Chem. 38*, 544−552.
62. Hlasta, D. J., Bell, M. R., Boaz, N. W., Court, J. J., Desai, R. C., Franke, C. A., Mura, A. J., Subramanyam, C., and Dunlap, R. P. (1994) *Bioorg. Med. Chem. Lett. 4* (15), 1801−1806.
63. Zimmerman, M., Morman, H., Mulvey, D., Jones, H., Frankshun, R., and Ashe, B. M. (1980) *J. Biol. Chem. 255* (20), 9848−9851.
64. Hedstrom, L., Moorman, A. R., Dobbs, J., and Abeles, R. H. (1984) *Biochemistry 23*, 1753−1759.
65. Krantz, A., Spencer, R. W., Tam, T. F., Thomas, E., and Copp, L. J. (1987) *J. Med. Chem. 30*, 591−597.
66. Krantz, A., Spencer, R. W., Tam, T. F., Liak, T. J., Copp, L. J., Thomas, E. M., and Rafferty, S. P. (1990) *J. Med. Chem. 33*, 464−479.

67. Kaiser, E. T. (1974) *Bayer-Symp. V,* 523−530.
68. Stoddard, B. L., Bruhnke, J., Porter, N., Ringe, D., and Petsko, G. A. (1990) *Biochemistry 29,* 4871−4879.
69. Koenigs, P. M., Faust, B. C., and Porter, N. A. (1993) *J. Am. Chem. Soc. 115,* 9371−9379.
70. Powers, J. C., Oleksyszyn, J., Narasimhan, L., Kam, C.-M., Radhakrishnan, R., and Meyer, E. F., Jr. (1990) *Biochemistry 29,* 3108−3118.
71. Chow, M. M., Meyer, E. F., Jr., Bode, W., Kam, C.-M., Radhakrishman, R., Vijayalakshmi, J., and Powers, J. C. (1990) *J. Am. Chem. Soc. 112,* 7783−7789.
72. Henderson, R. (1970) *J. Mol. Biol. 54,* 341−354.
73. Maveyraud, L., Massova, I., Birck, C., Miyashita, K., Samama, J.-P., and Mobashery, S. (1996) *J. Am. Chem. Soc. 118,* 7435−7440.
74. Ringe, D., Mottonen, J. M., Gelb, M. H., and Abeles, R. H. (1986) *Biochemistry 25,* 5633−5638.
75. Bürgi, H. B., Dunitz, J. D., and Shefter, E. (1973) *J. Am. Chem. Soc. 95,* 5066−5067.
76. Perona, J. J., Craik, C. S., and Fletterick, R. J. (1993) *Science 261,* 620−622.
77. Singer, P. T., Smalas, A., Carty, R. P., Mangel, W. F., and Sweet, R. M. (1993) *Science 259,* 620−622.

BI972499O